ELSEVIER

Coordination Chemistry Reviews 237 (2003) 65–76

COORDINATION CHEMISTRY REVIEWS

www.elsevier.com/locate/ccr

Structural studies on the dodecameric vanadium bromoperoxidase from *Corallina* species

Jennifer Littlechild *, Esther Garcia-Rodriguez

Schools of Chemistry and Biological Sciences, University of Exeter, Exeter EX4 4QD, UK

Received 25 January 2002; accepted 23 August 2002

Contents

Abstract

The vanadium bromoperoxidase enzymes (VBPO) are receiving considerable interest since they show increased stability over the more commonly used heme chloroperoxidase enzymes. The multisubunit vanadium enzymes described in this article are exceptionally stable and offer the potential to be exploited for industrial catalysts. The multisubunit enzyme from *Corallina officinalis* was first crystallised in Exeter in a cubic form with cell dimensions of over 300 Å. This made the structural solution a difficult problem (FEBS Lett. 359 (1995) 244). The structure of this enzyme has now been solved in our laboratory after its crystallisation in another more favourable tetragonal crystal form grown from a high concentration of phosphate (Acta Crystallogr. D 54 (1998) 454; J. Mol. Biol. 299 (2000) 1035). Recombinant vanadium haloperoxidase has recently been studied from the related *C. pilulifera* species. This enzyme has been purified and crystallised in the presence of high concentrations of phosphate, in a trigonal space group $P6_3$. The structure has been solved by molecular replacement using the wild-type *C. officinalis* structure as a model with which the *C. pilulifera* VBPO shows over 90% sequence identity.

Keywords: Vanadium bromoperoxidase; *Corallina* species; Vanadium haloperoxidase

1. Introduction

Haloperoxidases are named according to the most electronegative halogen that they oxidise. On the basis of the cofactor requirement these enzymes are classified into three groups as heme containing, vanadium containing and metal free haloperoxidases [4].

* Corresponding author. Tel.: +44-1392-263-468; fax: +44-1392-263-434

E-mail address: jalittlechild@exeter.ac.uk (J. Littlechild).

0010-8545/02/$ - see front matter
PII: S0010-8545(02)00226-6

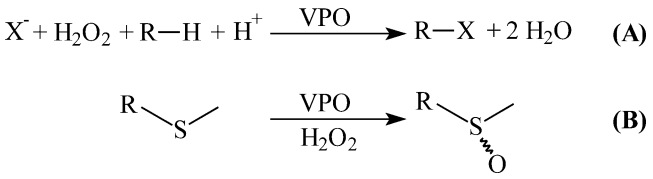

Scheme 1. (A) Halogenation reaction. (B) Sulfoxidation reaction. (VPO = vanadium haloperoxidase.)

Vanadium-dependent haloperoxidases catalyse the oxidative halogenation of several aromatic compounds in the presence of H_2O_2 and the appropriate halogen (Scheme 1A). The reaction is performed in a controlled and regiospecific way [5,6], making these enzymes valuable for industrial purposes. The enzyme also possesses sulfoxidation activity (Scheme 1B) [7]. The mechanism of these reactions is still a matter of controversy and experiments have been performed in order to determine the intermediates of the catalytic pathway.

A bromoperoxidase enzyme with an absolute requirement for vanadium was first isolated from the brown macro-algae *Ascophyllum nodosum* [8]. One molecule of vanadate per subunit was shown to be required for the enzyme activity. EPR studies [9] and K-edge X-ray absorption studies [10] on the bromoperoxidase from *A. nodosum* showed that the oxidation state of the metal was vanadium V. The redox state of the metal is not thought to change during turnover of the enzyme. It has been proposed that the function of the vanadium is to bind hydrogen peroxide to yield an activated peroxo intermediate, which is able to react with bromide to produce HOBr [11]. Vanadium-dependent haloperoxidase enzymes have also been isolated from a number of marine algae [12–22] and also from some lichens and fungi [23–26]. In algae the enzyme is located mainly in the extracellular part of the membrane, but it has also been detected inside the thallus [27]. The natural substrates and the role of the bromoperoxidase in the algae is thought to be involved in the polymerisation of polyphenols in order to hold the zygotes to the membrane during the reproductive cycle of the cell [28]. In the case of fungi and lichen the role of the enzyme remains unclear. However, suggestions have been made regarding its role in the degradation of plant material or in the organisms defence mechanism due to the biocidal effect of the organohalogens produced [29,30].

2. Methods

2.1. Enzyme purification

The haloperoxidase enzyme was extracted as previously described [2]. The macroalgae was collected from Ladrum Bay, Devon, UK in mid-winter when enzyme activity is maximal. The fresh, washed fronds were macerated using a mortar and pestle and suspended in buffer A (50 mM Tris/H_2SO_4, pH 8.0). The cell debris was removed by centrifugation at 4000 rpm for 20 min and the resulting crude protein extract was made 60% saturated with respect to ammonium sulphate (enzyme grade). After stirring for 1 h, the extract was centrifuged at 9600 rpm for 45 min. The pellet was resuspended in a minimum of buffer and dialysed overnight against buffer A containing 1 mM sodium vanadate. A FFQ™ Sepharose column (2.6×15 cm^2), equilibrated in buffer, was loaded with the dialysed sample. Protein was eluted with a linear gradient of 0–1 M KBr in buffer A over 10 bed volumes, with the vanadium bromoperoxidase enzyme (VBPO) activity eluting at 0.3 M KBr. Active fractions were pooled and concentrated using 80% ammonium sulphate. This was then loaded onto a Phenyl Sepharose CL-4B column (2.6×15 cm^2) which had been equilibrated with 10% ammonium sulphate in buffer A. Protein was eluted with a negative linear gradient from 10 to 0% ammonium sulphate, with the VBPO activity eluting between 4 and 0% ammonium sulphate. Active fractions were again pooled and concentrated using 80% ammonium sulphate. The pellet was resuspended in a minimum of buffer A and applied to a Sepharose 6B gel filtration column (1.5×30 cm^2). Fractions with activity were collected and applied to a Sephacryl S-1000HR gel filtration column (2.6×25 cm^2). Active fractions from this final step were pooled and concentrated by centrifugation using Amicon centricons (10 kD cut-off). The purified protein sample ran as a single band on SDS-PAGE with a molecular weight of 64 kD.

The recombinant *Corallina pilulifera* enzyme was kindly provided by Professor Y. Izumi and Dr T. Ohshiro, Tottori University, Japan. The enzyme was over-expressed in yeast and purified by a modification of the method previously described [31]. The molecular weight of the monomer has been determined to be 65.3 kD.

2.2. Crystallisation and data collection

The VBPO from *C. officinalis* has been crystallised in two different forms [1,2]. A cubic crystal form was grown in the presence of vanadium and a tetragonal form was grown from ammonium phosphate. The first crystals to be grown were cubic and the second crystal form was tetragonal. The cubic crystals grow from 30% PEG 6000, 50 mM Tris/H_2SO_4 buffer pH 6.8 and 0.4 M KCl in about 1–2 weeks and are typically $0.3 \times 0.3 \times 0.3$ mm in dimension. The crystals diffract beyond 2.5 Å resolution and are in the cubic space group $I23$ with cell dimensions $a = b = c = 310$ Å. The second crystals grow from 0.1 M Tris/HCl and 2 M ammonium dihydrogen

phosphate at pH 5. The cell dimensions for this crystal form are $a = b = 201.9$, $c = 178.7$ Å, $\alpha = \beta = \gamma = 90^\circ$ and the space group has been determined to be $P4_222$.

To solve the structure of the *C. officinalis* VBPO native data were collected from a single crystal of the tetragonal form to 2.3 Å resolution at the at EMBL X31 Hamburg synchrotron. The crystal used for a native data collection was later soaked for 1 h in mother liquor containing 10 mM mercury acetate. Derivative data were collected to 2.5 Å resolution on the same beamline at 0.99 Å wavelength, in order to optimise the anomalous signal of the mercury [3].

The VBPO from *C. pilulifera* has also been crystallised in two different forms based on the crystallisation conditions described for *C. officinalis* VBPO, with only slight variations in the precipitant concentration. The conditions that had produced tetragonal crystals for *C. officinalis* VBPO produced a trigonal $P6_3$ crystal form with the *C. pilulifera* VBPO, which grew within 1 week. Cubic crystals were also grown for *C. pilulifera* VBPO using KBr as the crystallisation salt and with 1 mM sodium vanadate to activate the enzyme. These crystals have been determined to be in the space group $P2_13$. Data have been collected to 2.2 Å for the trigonal crystal form of the *C. pilulifera* VBPO on the X11 beamline at the EMBL Synchrotron, Hamburg. The cell parameters are $a = b = 185.95$ Å, $c = 180.28$ Å, $\alpha = \beta = 90^\circ$, $\gamma = 120^\circ$. The data for the cubic crystal form of *C. pilulifera* VBPO was collected on station BW7a at the EMBL Synchrotron, Hamburg. The unit cell has dimensions $a = b = c = 195.436$ Å, $\alpha = \beta = \gamma = 90^\circ$. Only the trigonal crystal form of the *C. pilulifera* VBPO was successfully frozen with cryoprotectants during data collection.

2.3. Structure solution

The original structure of the tetragonal form of the *C. officinalis* enzyme was solved using a single derivative and the pseudosymmetry of the subunit arrangement. The native structure of the enzyme is a dodecamer [3] that is in agreement with earlier sedimentation studies [32] and electron microscopy studies ([33], Sabil and Littlechild, unpublished results). The complete amino acid sequence of the *C. officinalis* VPBO was unknown at the time when the structure was determined. The partial amino acid sequence information that was available showed that the *C. officinalis* VPBO was closely related to the two VBPOs of the related red algae *C. pilulifera* [31] with over 90% identity for the five regions that had been protein sequenced (Rush and Littlechild, unpublished data). The two amino acid sequences of the *C. pilulifera* VBPO enzymes were used as a basis for the side chain assignments in the *C. officinalis* VBPO X-ray structure. The electron density maps were calculated using phases from the VBPO enzyme structure with zero side chain occupancy of the residue in question in order to resolve the sequence ambiguities in the primary structure of the *C. officinalis* enzyme. The resulting 2Fo–Fc and Fo–Fc maps were inspected in all six subunits in the asymmetric unit (program O, [34]). These maps were consistent with the consensus sequence between the two *C. pilulifera* enzymes for 534 amino acids out of 595 (89.7% of total). Ten amino acids in each subunit were assigned to a different residue type from the consensus sequence and one or two residue insertions found in the *C. pilulifera* and not observed in the *C. officinalis* electron density maps were accommodated [3]. We have subsequently cloned the *C. officinalis* enzyme (Coupe and Littlechild, unpublished data) and are in a position to compare the sequence derived from the X-ray structure of this enzyme with the sequence derived from the DNA sequence (Fig. 1).

The structure of the related *C. pilulifera* VBPO was solved using molecular replacement (program AMoRe [35], CCP4 package [36]) with the structure of the monomer of *C. officinalis* VBPO as search model. Four solutions were found to this model, corresponding to the four molecules in the asymmetric unit. Rebuilding of the model was performed using the program O [34] to create a model with the correct sequence and to rebuild the parts of the structure where insertions should appear according to the sequence number 1 of *C. pilulifera* [31]. Examination of the omit maps allowed the building of these insertions in the loop region formed by amino acids 45–52. The refinement was performed using the program REFMAC [37] (CCP4 package, [36]) and the molecules of solvent were assigned using Quanta™ [38]. The structural figures have been created using the program BobScript [39] and rendered with Raster3D [40] unless otherwise stated.

3. The monomer structure

The *Corallina* VBPO (CVBPO) monomer measures ca. 85 × 56 × 55 Å in size. It is folded into a single α+β type domain of 595 amino acids for *C. officinalis* VBPO and 597 amino acids for *C. pilulifera* VBPO. The first 10 N-terminal amino acids point away from the body of the domain that is composed of nineteen α-helices from 6 to 26 amino acids in length. There are also 8 3_{10} helices and 14 β-strands. The β-strands are mainly involved in β-hairpins. One of the surfaces of the subunit is flat.

A divalent cation is bound in an α-helix/β-strand motif formed between the amino acids 359 and 366 (*C. officinalis* VBPO numbering). This is discussed in more detail below (Fig. 2).

Another characteristic of this enzyme is the acidity of its molecular surface. In contrast, the residues involved in the active site cleft are mainly basic, leading to a high difference in the potential of the surface as it is shown in

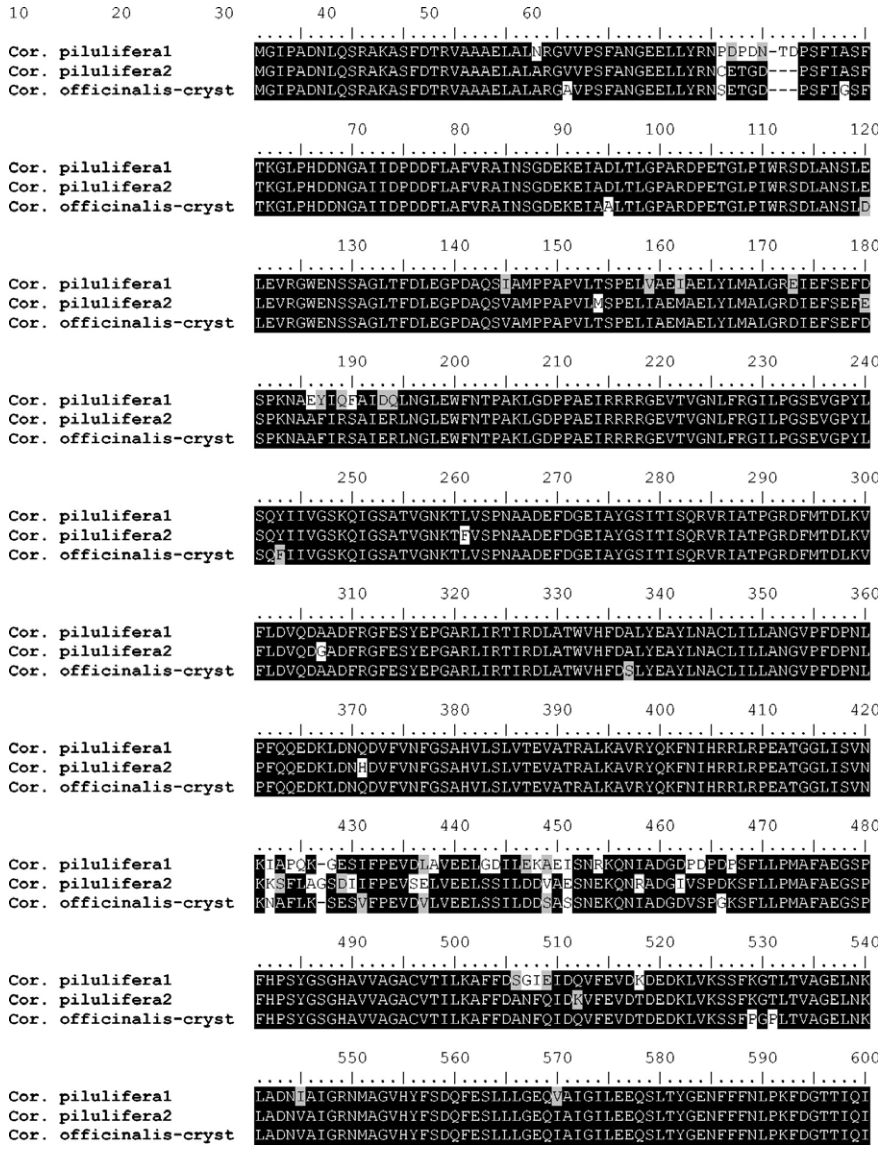

Fig. 1. Sequence alignment of the *Corallina* VBPOs. Conserved amino acids are shown with a black background, similar amino acids are shown in grey. The figure was created with the program BioEdit [51].

Fig. 3. The isoelectric point of the *Corallina* VBPO has been determined to be 4.5 [1], which is consistent with this data.

4. The dimer structure

The CVBPO dimer structure is shown in Fig. 4. The flat surfaces of the two subunits complement each other covering an area of 5260 Å^2 or 20.5% of the subunit solvent accessible surface. The residues 123–124 from one subunit and 368–369 from the other subunit in the dimer form a parallel two-stranded β-sheet. The β-hairpins 270–273 and 276–279 from each subunit in the dimer form an antiparallel four-stranded β-sheet. The vanadate binding site is located at the bottom of the active site cleft, which is about 20 Å deep and 14 Å wide. The active site cleft is formed from residues of two different subunits in the dimer.

The residues of one subunit form the bottom of the cleft and the top of the cleft is formed predominantly from the residues of the other subunit of the dimer. The involvement of residues from the neighbouring subunit in the active site cleft would suggest that the CVBPO dimer is required to maintain selectivity and regiospecificity for halogenation of organic substrates [5,6], despite the fact that all vanadate binding residues are coming from one subunit.

Fig. 2. Ribbon representation of the monomer of *C. pilulifera* VBPO. The phosphate group (purple) and the calcium atom (cyan) are shown in space-filling mode.

5. The dodecamer structure of the native enzyme

The CVBPO dodecamer measures ca. 150 Å in diameter. Twelve subunits are arranged with 23 cubic point group symmetry (Fig. 5). This symmetry has now been observed in several other enzyme structures—a DNA protection protein Dps from *Escherichia coli* [41], an ornithine carbamoyltransferase from *Pyrococcus furiosus* [42], a type II dehydroquinase from *Streptomyces coelicolor* [43], a urease from *Helicobacter pylori* [44], a ferritin from *Listeria innocua* [45] and a 3-dehydroquinate dehydratase from *Mycobacterium tuberculosis* [46].

In the *Corallina* VBPOs, each of the cubic faces is made up of a homodimer. The N-terminal region of each subunit contributes to the formation of the central cavity. The diameter of this cavity is about 26 Å and it does not have any specific charge or hydrophobic properties and is therefore unlikely to bind metals. The interaction of the helices to form the cavity is proposed to have a structural role.

An additional 3245 $Å^2$ of the solvent accessible area of each subunit is buried upon dodecamer formation from dimers. This gives an overall figure of 8505 $Å^2$ for the buried area for each subunit, which amounts to 33.2% of its surface. Each subunit makes at least one H-bond with nine other subunits within the dodecamer.

6. The active site of CVBPO

The vanadium-binding site in the phosphate form of the *Corallina* VBPO structures is located on the bottom of a deep cavity formed by residues from both subunits. The bottom of the cleft is formed by the residues of helices α10, α11, α14, α17, α18, α19 of one subunit. The top of the cleft is formed by the residues of helix α9 and some loops from the same subunit and helices α11, α12

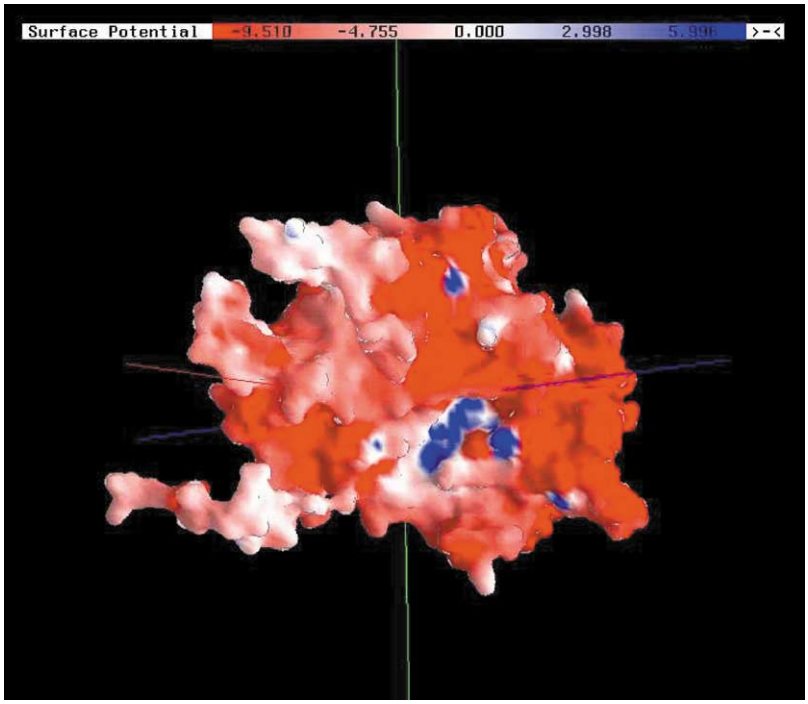

Fig. 3. Surface potential of the monomer in *Corallina* VBPOs. The active site cleft shows high positive potential in relation to the rest of the enzyme. The figure was prepared with the program GRASP [52].

and α3, the β-hairpin (251–253 and 256–258) and the divalent cation binding motif of the neighbouring subunit. The long helix α11 contributes its residues to the active site clefts of both subunits.

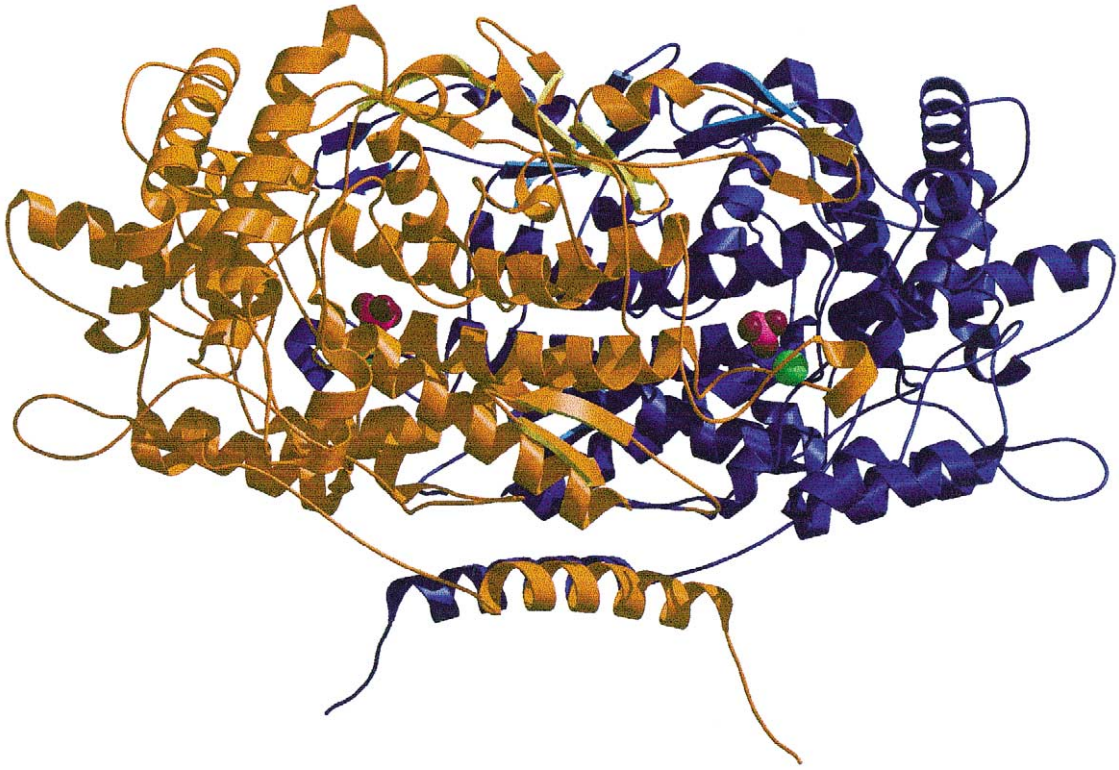

Fig. 4. The catalytic dimer of *C. pilulifera* VBPO. A molecule of phosphate (in purple) represented in space-filling mode can be seen in each of the active sites. One atom of calcium (in green) from the other subunit sits close to the active site cleft.

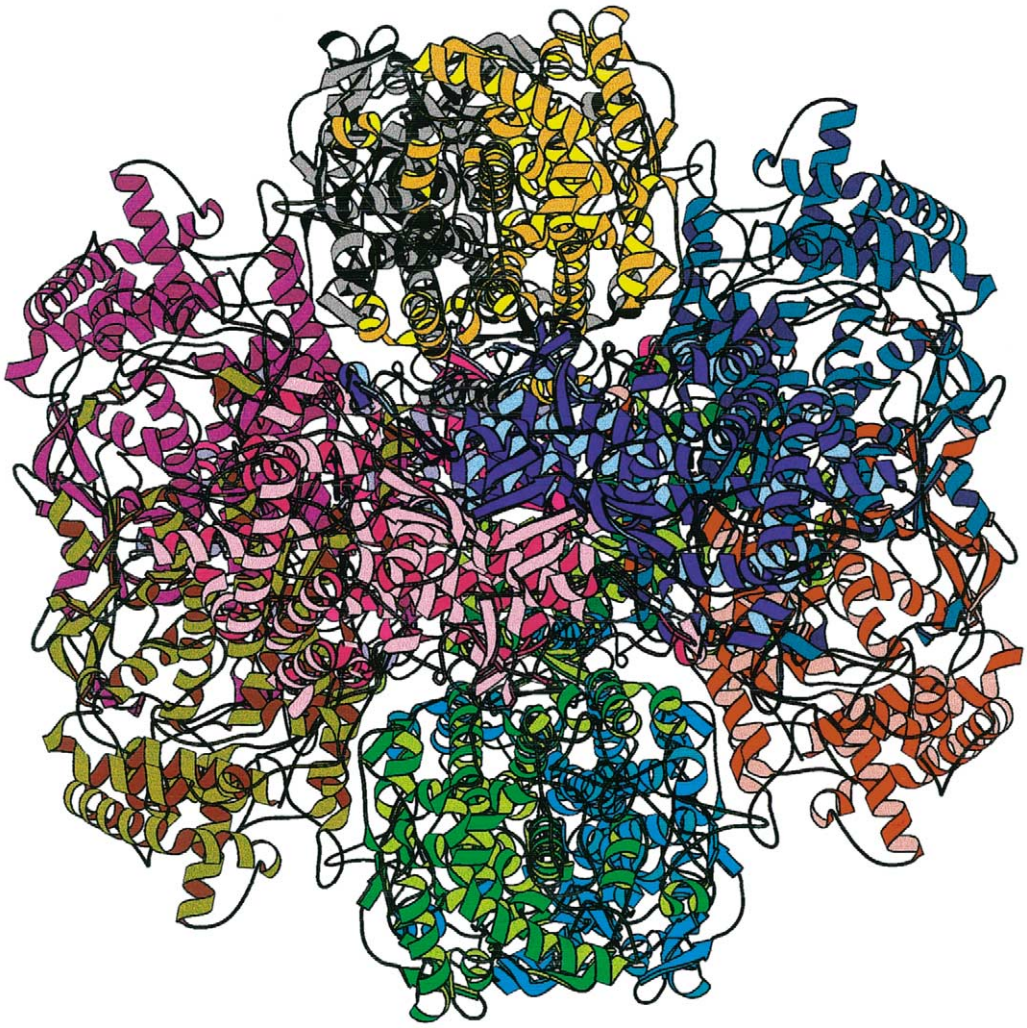

Fig. 5. The dodecamer of the *C. pilulifera* VBPO enzyme, as viewed from the twofold axis.

In the structure initially solved the active site is occupied by inorganic phosphate, coordinated in a tetrahedral geometry as is shown in Fig. 6A. The phosphate is located at the N-terminus of the helix α17 at the bottom of the cleft and is stabilised by its dipole moment and H-bonds with Ser483 OG, Gly484 N and His485 ND1. The His551, which is proposed to make a covalent bond to the vanadium, is H-bonded to one of the phosphate oxygen atoms. Additionally, the phosphate is forming salt bridges with Lys398 (helix α13), Arg406 (helix α14) and Arg545 (helix α18). In *C. pilulifera* VBPO a second molecule of phosphate is H-bonded to the main phosphate as illustrated in the figure, which is probably the result of the high phosphate concentration used during crystallisation of the enzyme.

There are several hydrophobic patches and charged residues that could provide binding sites for the organic substrates. Attempts to co-crystallise CVBPO with various known organic substrates or halogen ions or to obtain the complexes by soaking of the crystals are in progress.

Divalent cations thought to be Mg^{2+} in *C. officinalis* VBPO and Ca^{2+} in *C. pilulifera* VBPO bind close to the subunit interface in the dimer on the top of the active site cleft. Main chain oxygen atoms of Phe359, Gln361 and Gln368 and carboxyl groups of Asp363 and Asp366 coordinate the metal in both species. The distance between the divalent cation of one subunit of the dimer and the phosphorus of the inorganic phosphate bound at the active site of the other subunit is 19 Å. Divalent cations seem to be necessary to maintain the structure of the active site cleft.

7. Differences between *C. officinalis* and *C. pilulifera* VBPO enzymes

Regardless of the high sequence similarity observed between the two *Corallina* VBPO enzymes some features

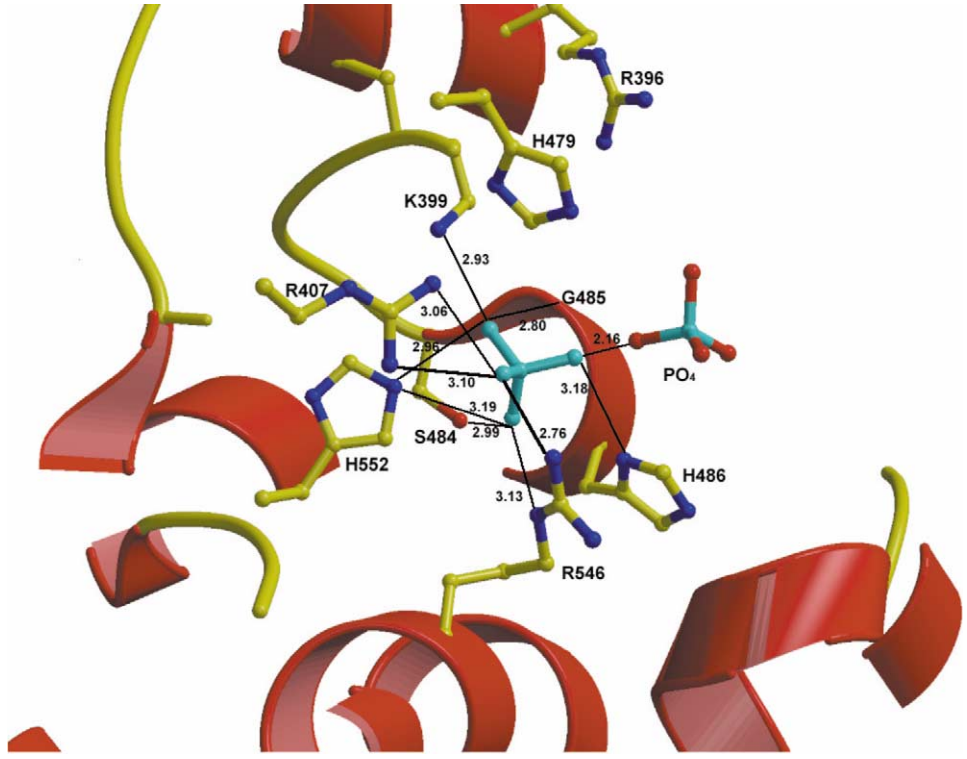

(a)

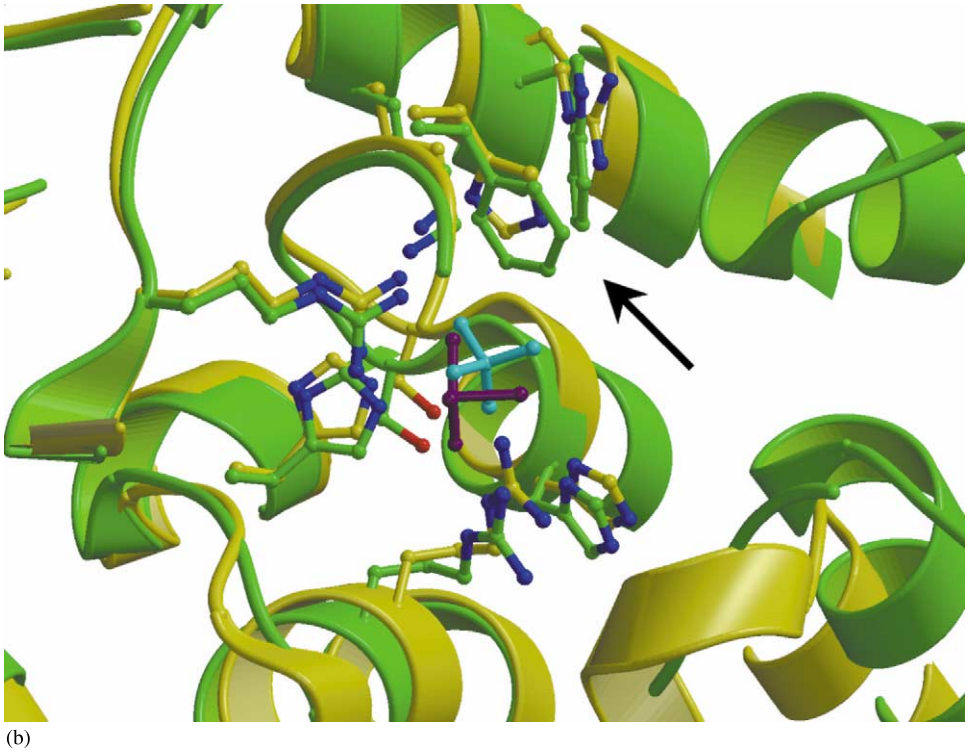

(b)

Fig. 6. (a) The active site of *C. pilulifera* VBPO showing the residues involved in direct phosphate binding and structure of the active site as ball-and-stick. The main phosphate is shown in cyan. Distances are in angstroms. (b) Superposition of the active sites of chloroperoxidase from *Cur. inaequalis* (in green) and *C. pilulifera* VBPO (in yellow). The residues surrounding the main phosphate (cyan) or vanadate (purple) are shown in ball-and-stick. His478 and Arg395 are substituted in their positions by Phe397 and Trp350 in the chloroperoxidase, respectively and as indicated by an arrow.

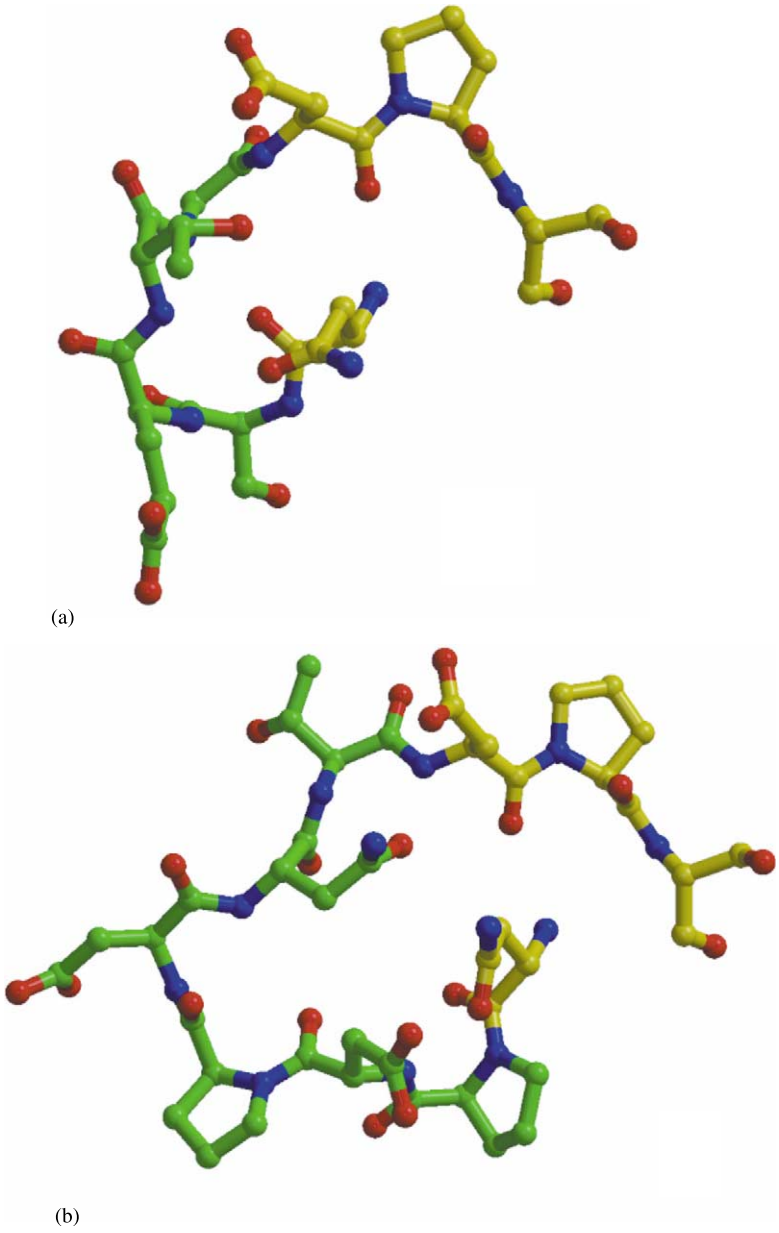

Fig. 7. Comparison of the loop 45–50 from *C. officinalis* VBPO (a) and *C. pilulifera* VBPO (b), in which the insertions can be observed. The region of amino acid sequence variation is shown in green.

of the structure are found to differ where sequence variations or insertions are most frequent. These differences do not affect the overall structure of the dimers and subsequent dodecameric arrangement of the enzyme. There are no changes observed within the active site cleft.

A new conformation of the loop formed by amino acids 45–50 is observed in the VBPO from *C. pilulifera*. The insertion of an asparagine and a threonine in this region was clearly visible in the omit maps, and the final structure of this region is shown in Fig. 7 in comparison to the corresponding region in VBPO from *C. officinalis*.

Another interesting change is observed in the loop constituted by the amino acids 456–463. Differences in the sequence in this region cause a completely different position of this loop, which folds in the opposite direction to that found in the *C. officinalis* structure, as is illustrated in the Fig. 8. This loop is situated on the surface of the enzyme, and it can be seen in the picture that the structure converges in both enzymes in the proximity of the active site, which appears to be the

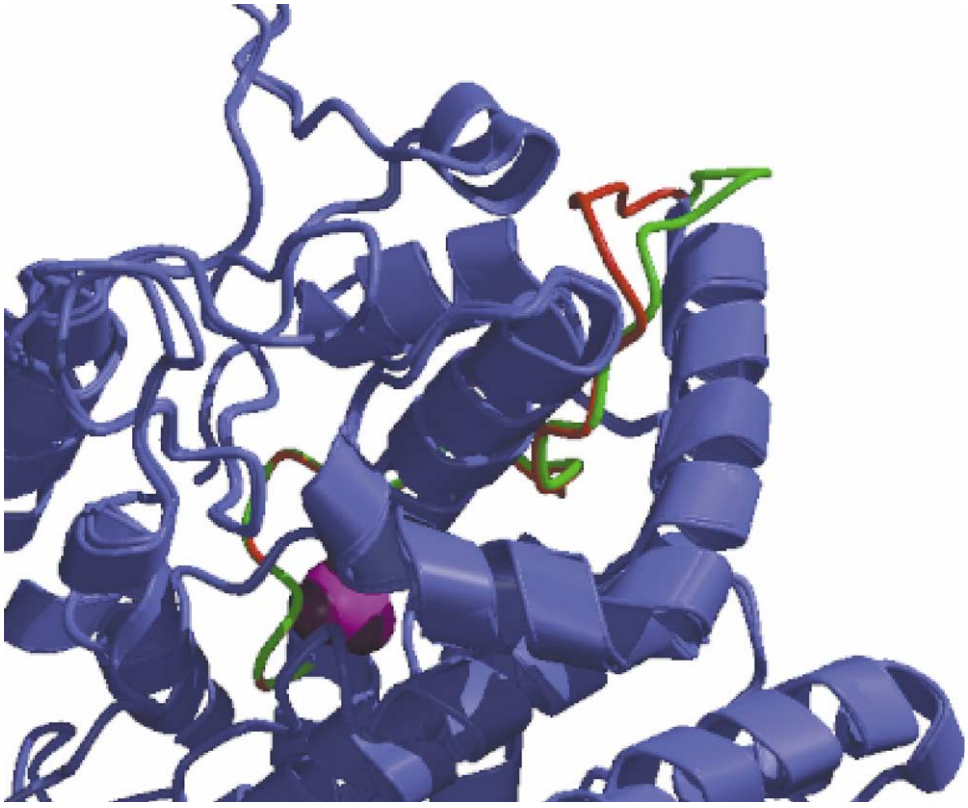

Fig. 8. Superposition of *C. officinalis* VBPO 456–463 loop (red) and the *C. pilulifera* VBPO equivalent (green). The phosphate bound in the active site is represented in space-filling mode.

same in both enzyme structures.

The calcium atom is surrounded by the same amino acids that are found in the *C. officinalis* VBPO enzyme structure and the structure is this region is conserved. It is not clear why the bound cation is different between the two *Corallina* species but could be the result of the different isolation procedures or the fact that the one of the enzymes is recombinant and the other is not.

8. Comparison with other vanadium haloperoxidases

The structure of the chloroperoxidase from the fungus *Cur. inaequalis* [47], which is a two domain protein, can be superimposed with the CVBPO dimer. Many of the α-helices of each chloroperoxidase domain are structurally equivalent to the α-helices in the *Corallina* VBPO dimer. This suggests an evolutionary relationship between the *Corallina* VBPO and the chloroperoxidase. The *Corallina* VBPO dimer and chloroperoxidase monomer can be superimposed with a rms deviation of 1.9 Å for 259 matching Cα atoms. It is proposed that the CVBPO represents an ancestral enzyme with two subunits required to form the catalytic cleft while the chloroperoxidase has undergone gene duplication. The chloroperoxidase has lost the catalytic function of its N-terminal domain. It would appear that the chloroperoxidase C-terminal domain has retained the structure and residues related to catalytic functions and has lost most of the features related to a second active site during evolution. On the contrary, the N-terminal domain retained mainly features that contribute to the active site cleft in the catalytic domain and lost features of its own active site. However, the number of residues per catalytic site has remained similar (595/97 in *Corallina* VBPO and 609 in the chloroperoxidase).

Since the structure of the CVBPO was solved a related VBPO from *A. nodosum* (AVBPO) also became available [48]. AVBPO and *Corallina* VBPO enzymes have 33% amino acid sequence identity. The long α-helices that make up the core of the molecule are structurally conserved between the two enzymes. Many of the small helices and β-strands that are on the surface of the enzymes differ between the two structures and the number and location of the β-strands is also different. The divalent cations are not found in the AVBPO structure and the α-helix/β-strand cation binding feature of *Corallina* VBPO is not observed in the *A. nodosum* enzyme, which has a three residue deletion in this region.

Both AVBPO and *Corallina* VBPO show high thermostability as well as stability to organic solvents and to high concentrations of hydrogen peroxide. The thermostability of these enzymes, which come from mesophilic species could be due to an adaptation to the harsh

environmental conditions of overheating and dehydration that the algae endure at low tide. It seems that the AVBPO and *Corallina* VBPO have developed different mechanisms of stability. In the dimeric AVBPO enzyme the cysteine residues are involved in three intersubunit and one intrasubunit disulphide bonds which make a significant contribution to the enzyme stability. None of these cysteines residues are conserved in CVBPO which has two other cysteine residues that are located far apart and are in the reduced form. The stability of CVBPO seems to result from the high dodecameric oligomerisation that buries an extra 12% of the subunit solvent accessible area and from the binding of the divalent cations described above.

All of the residues involved in the vanadate binding are conserved between the two algal bromoperoxidases and the vanadium chloroperoxidase from the fungus *Cur. inaequalis*. Only five residues out of seventeen lining the wall of the active site cavity and not involved in the vanadate binding are conserved between *Corallina* VBPO and AVBPO. None of these five residues is structurally conserved in the *Cur. inaequalis* chloroperoxidase structure. His478 is located at the position of Phe397 in *Cur. inaequalis* (Fig. 6B), which was suggested to bind the chloride in the chloroperoxidase active site [47]. This substitution and H-bonding of Asp333 (Asp278) to the catalytic His485 (His418) were suggested to be the reasons for a preference for bromination rather than chlorination for AVBPO [48] and indeed His478 and Asp333 or their equivalents are conserved in all VBPOs. An active site serine was suggested as a possible candidate to form a carbon–bromine covalent bond from EXAFS studies [49]. However, the solvent accessibility of this Ser483 in CVBPO (Ser416 in AVBPO) seems to be low in the phosphate-bound form of the enzyme. The significant structural changes within the active site during the catalytic cycle that would make it accessible have been ruled out for the chloroperoxidase enzyme on the basis of structural studies on mutant proteins [50].

Only three hydrophilic residues and no charged residues except those involved in the vanadate binding are observed within 7.5 Å from the vanadate O^4 oxygen in the *A. nodosum* structure [48]. There are three charged residues—within approximately the same sphere in *Corallina* VBPO. These residues could affect the substrate specificity and stereoselectivity of the reaction.

The structure factors and refined coordinates of the *C. officinalis* and *C. pilulifera* bromoperoxidase have been deposited with the Brookhaven Protein Data Bank. The access code for *C. officinalis* is 1QHB and the *C. pilulifera* is in the process of deposition.

References

[1] C. Rush, A. Willetts, G. Davies, Z. Dauter, H. Watson, J.A. Littlechild, FEBS Lett. 359 (1995) 244.
[2] A.A. Brindley, A.R. Dalby, M.N. Isupov, J.A. Littlechild, Acta Crystallogr. D 54 (1998) 454.
[3] M. Isupov, A. Dalby, A. Brindley, Y. Izumi, T. Tanabe, J. Littlechild, J. Mol. Biol. 299 (2000) 1035.
[4] J. Littlechild, Curr. Opin. Chem. Biol. 3 (1999) 28.
[5] P. Coughlin, S. Roberts, C. Rush, A. Willetts, Biotech. Lett. 15 (1993) 907.
[6] J.S. Martinez, G.L. Carroll, R.A. Tschirret-Gutz, G. Altenhoff, R.O. Little, A. Butler, J. Am. Chem. Soc. 123 (2001) 3289.
[7] M. Andersson, A. Willets, S. Allenmark, J. Org. Chem. 62 (1997) 8455.
[8] H. Vilter, Phytochemistry 23 (1984) 1387.
[9] E. de Boer, K. Boon, R. Wever, Biochemistry 27 (1988) 1629.
[10] J. Hormes, U. Kuetgens, R. Chauvistre, W. Schreiber, N. Anders, H. Vilter, D. Rehder, C. Weidemann, Biochim. Biophys. Acta 956 (1988) 293.
[11] A. Messerschmidt, L. Prade, R. Wever, Biol. Chem. 378 (1997) 309.
[12] M. Almeida, M. Humanes, R. Melo, J.A. Silva, J.J.R.F. da Silva, H. Vilter, R. Wever, Phytochemistry 48 (1998) 229.
[13] M.G. Almeida, M. Humanes, R. Melo, J.A. Silva, J.J.R.F. da Silva, R. Wever, Phytochemistry 54 (2000) 5.
[14] V.A. Bukin, A.K. Gladiliin, V.Y. Levitskii, O.A. Guseva, A.V. Levashov, Appl. Biochem. Microbiol. 33 (1997) 241.
[15] I. Hara, T. Sakurai, J. Inorg. Biochem. 72 (1998) 23.
[16] N. Itoh, Y. Izumi, H. Yamada, Biochem. Biophys. Res. Commun. 131 (1985) 428.
[17] P. Jordan, H. Vilter, Biochim. Biophys. Acta 1073 (1991) 98.
[18] B.E. Krenn, H. Plat, R. Wever, Biochim. Biophys. Acta 912 (1987) 287.
[19] M.L. Shang, R.K. Okuda, D. Worthen, Phytochemistry 37 (1994) 307.
[20] H.S. Soedjak, A. Butler, Biochemistry 29 (1990) 7974.
[21] H. Yu, J.W. Whittaker, Biochem. Biophys. Res. Commun. 160 (1989) 87.
[22] E. de Boer, M.G.M. Tromp, H. Plat, G.E. Krenn, R. Wever, Biochim. Biophys. Acta 872 (1986) 104.
[23] P. Barnett, W. Hemrika, H.L. Dekker, A.O. Muijsers, R. Renirie, R. Wever, J. Biol. Chem. 273 (1998) 23381.
[24] B.E. Krenn, H. Plat, R. Wever, J. Royal Neth. Chem. Soc. 106 (1987) 407.
[25] T. Rezanka, V. Dembitsky, Phytochemistry 50 (1999) 97.
[26] J.W.P.M. Van Schijndel, E.G.M. Vollenbroek, R. Wever, Biochim. Biophys. Acta 1161 (1993) 249.
[27] B.E. Krenn, M.G. Tromp, R. Wever, J. Biol. Chem. 264 (1989) 19287.
[28] V. Vreeland, J.H. Waite, L. Epstein, J. Phycol. 34 (1998) 1.
[29] S.L. Neidleman, J. Geigert, Biohalogenation: Principles, Basic Roles and Applications, Ed. Ellis Horwood Ltd, Chichester, 1986, p. 13.
[30] B.H. Simons, P. Barnett, E.G.M. Vollenbroek, H.L. Dekker, A.O. Muijsers, A. Messerschmidt, R. Wever, Eur. J. Biochem. 229 (1995) 566.
[31] M. Shimonishi, S. Kuwamoto, H. Inoue, R. Wever, T. Ohshiro, Y. Izumi, T. Tanabe, FEBS Lett. 428 (1998) 105.
[32] D.J. Sheffield, T.R. Harry, A.J. Smith, L.J. Rogers, Phytochemistry 32 (1993) 21.
[33] N. Itoh, Y. Izumi, H. Yamada, J. Biol. Chem. 261 (1986) 5194.
[34] T.A. Jones, J.Y. Zou, S.W. Cowan, M. Kjelgaard, Acta Crystallogr. A 47 (1991) 110.
[35] J. Navaza, Acta Crystallogr. D 50 (1994) 157.

[36] Collaborative Computational Project, Number 4, Acta Crystallogr. D 50 (1994) 760.
[37] G.N. Murshudov, A.A. Vagin, E.J. Dodson, Acta Crystallogr. D 53 (1997) 240.
[38] 'Quanta2000™' Molecular Simulations Inc., 2001.
[39] R.M. Esnouf, Acta Crystallogr. D 55 (1999) 938.
[40] E.A. Merritt, D.J. Bacon, Methods Enzymol. 277 (1997) 505.
[41] R.A. Grant, D.J. Filman, S.E. Finkel, R. Kolter, J.M. Holge, Nat. Struct. Biol. 5 (1998) 294.
[42] V. Villeret, B. Clantin, C. Tricot, C. Legrain, M. Roovers, V. Stalon, N. Glansdorff, J. Van Beeumen, Proc. Natl. Acad. Sci. USA 95 (1998) 2801.
[43] A.W. Roszak, T. Krell, D.A. Robinson, I.S. Hunter, M. Fredrickson, C. Abell, J.R. Coggins, A.J. Lapthorn, Structure 10 (2002) 493.
[44] N.C. Ha, S.T. Oh, J.Y. Sung, K.A. Cha, M. Hyung Lee, B.H. Oh, Nat. Struct. Biol. 8 (2001) 505.
[45] A. Ilari, S. Stefanini, E. Chiancone, D. Tsernoglou, Nat. Struct. Biol. 7 (2000) 38.
[46] D.G. Gourley, A.K. Shrive, I. Polikarpov, T. Krell, J.R. Coggins, A.R. Hawkins, N.W. Isaacs, L. Sawyer, Nat. Struct. Biol. 6 (1999) 521.
[47] A. Messerschmidt, R. Wever, Proc. Natl. Acad. Sci. USA 93 (1996) 392.
[48] M. Weyand, H.J. Hecht, M. Kiess, M.F. Liaud, H. Vilter, D. Schomburg, J. Mol. Biol. 293 (1999) 595.
[49] H. Dau, J. Dittmer, M. Epple, J. Hanss, E. Kiss, D. Rehder, C. Schulzke, H. Vilter, FEBS Lett. 457 (1999) 237.
[50] S. Macedo-Ribeiro, W. Hemrika, R. Renirie, R. Wever, A. Messerschmidt, J. Biol. Inorg. Chem. 4 (1999) 209.
[51] T.A. Hall, Nucl. Acids Symp. Ser. 41 (1999) 95.
[52] A. Nicholls, K. Sharp, B. Honig, Proteins Struct. Func. Gen. 11 (1991) 281.